Supershear Earthquakes: Their Occurrence and Importance for Seismic Hazard, Early Warning, and Design Standards

Ahmed Elbanna[*1,2,3], Mohamed Abdelmeguid[4], Domniki Asimaki[5], Napat Tainpakdipat[1], Grigorios Lavrentadis[5], Ares Rosakis[4], and Yehuda Ben-Zion[6,3]

Abstract

Strike-slip faults—where tectonic plates grind past each other horizontally—are a defining feature of many densely populated continental seismic zones worldwide, including the San Andreas fault system in California, the North and East Anatolian faults in Türkiye, and the Sagaing fault in Myanmar (Burma). Although their lateral motion has long been recognized, a growing body of global evidence is now highlighting a more hazardous aspect of these systems: supershear earthquakes—fast propagating ruptures that exceed the speed of shear waves and can cause disproportionately intense shaking and destruction. Four of the last six M_w 7.0+ earthquakes on strike-slip faults have been recognized as supershear events, including the damaging M_w 7.7 Myanmar and the M_w 7.8 Pazarcik earthquakes, highlighting the need to confront the potential implications of such future events.

Cite this article as Elbanna, A., M. Abdelmeguid, D. Asimaki, N. Tainpakdipat, G. Lavrentadis, A. Rosakis, and Y. Ben-Zion (2025). Supershear Earthquakes: Their Occurrence and Importance for Seismic Hazard, Early Warning, and Design Standards, *Seismol. Res. Lett.* **XX**, 1–5, doi: 10.1785/0220250118.

Supershear: The Seismic Speed Trap

Traditionally, estimates of average rupture speed in large earthquakes have led to the assumption that most strike-slip earthquakes propagate at sub-Rayleigh speeds—slower than shear waves. Such ruptures tend to radiate energy to the volume around the faults diffusely, and their strongest shaking is often directed perpendicular to the fault. But supershear ruptures are different. When the rupture velocity exceeds the shear-wave speed, it generates shear Mach cones—intense, focused shear shock fronts analogous to sonic booms from supersonic jets (Fig. 1). These shock waves concentrate elevated shaking along the fault strike, especially in the forward direction of rupture propagation, amplifying both the horizontal and vertical ground motions. This produces ground shaking that spreads from the hypocenter faster than typical sub-Rayleigh events, with stronger and more damaging amplitudes—first in the direction of rupture propagation involving the supershear pulse, followed by fault normal shaking linked to the trailing Rayleigh pulse. Structures within the affected area experience not only amplified shaking but also increased torsional loading due to the "double punch" effect delivered by the leading supershear pulse and its trailing Rayleigh wave (Mello *et al.*, 2010). Such loading scenarios are overlooked so far in most seismic hazard assessments, and standard design procedures that for near-fault structures assign the strongest ground-motion component to the fault normal direction (ASCE/SEI, 2022). These effects are further magnified when rupture speeds accelerate abruptly or when the rupture maintains supershear velocities over extended fault segments. In addition, the weaker attenuation of shock wavefronts in supershear events (Dunham and Bhat, 2008; Mello *et al.*, 2010) increases the spatial extent of strong shaking, thereby raising the likelihood of triggering secondary hazards and causing infrastructure failures across broader regions. Although empirical

1. Department of Civil and Environmental Engineering, University of Illinois Urbana Champaign, Urbana, Illinois, U.S.A., https://orcid.org/0009-0007-1681-8957 (NT); 2. Beckman Institute of Advanced Science and Technology, University of Illinois Urbana Champaign, Urbana, Illinois, U.S.A.; 3. Statewide California Earthquake Center, University of Southern California, Los Angeles, California, U.S.A., https://orcid.org/0000-0002-9602-2014 (YB-Z); 4. Graduate Aerospace Laboratories, California Institute of Technology, Pasadena, California, U.S.A., https://orcid.org/0000-0002-3985-1721 (MA); https://orcid.org/0000-0003-0559-0794 (AR); 5. Department of Mechanical and Civil Engineering, California Institute of Technology, Pasadena, California, U.S.A., https://orcid.org/0000-0002-3008-8088 (DA); https://orcid.org/0000-0001-6546-1340 (GL); 6. Department of Earth Sciences, University of Southern California, Los Angeles, California, U.S.A.

*Corresponding author: elbanna2@illinois.edu

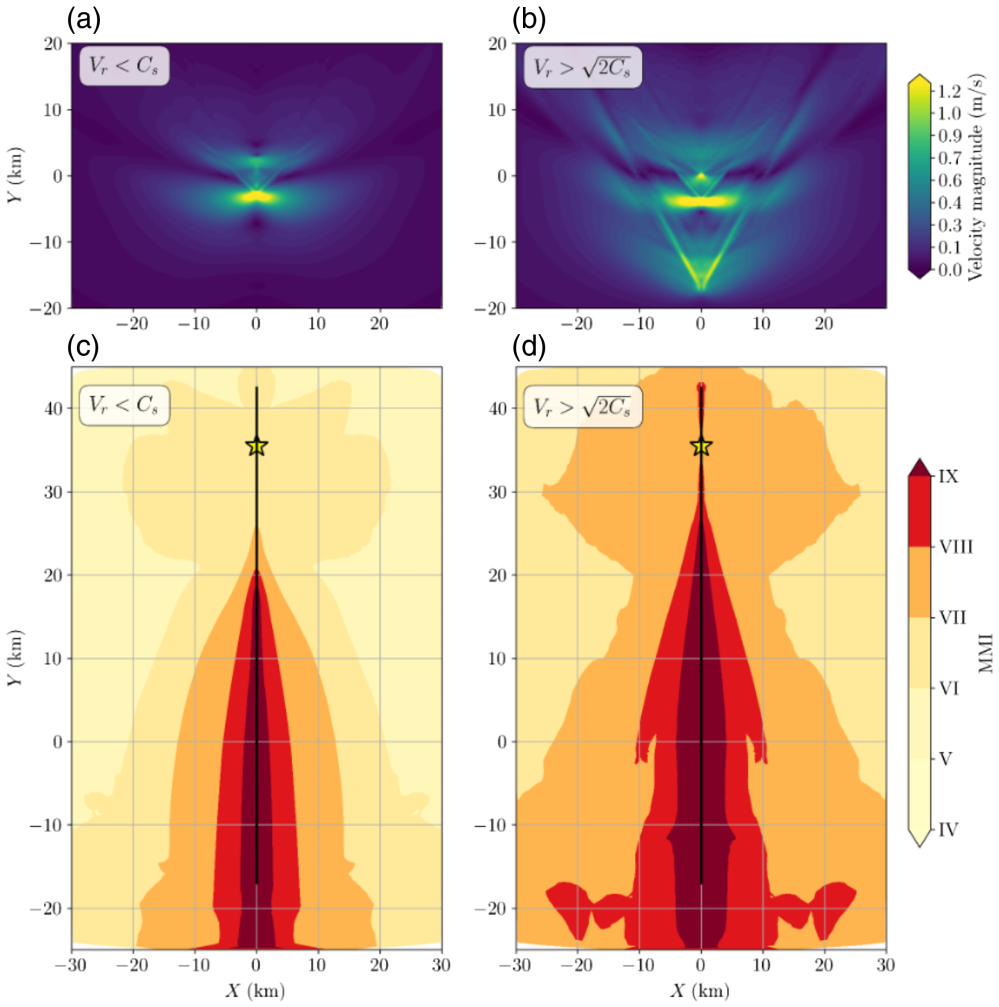

Figure 1. Comparison between simulated sub-Rayleigh and supershear earthquakes with magnitudes M_w 7.15 and 7.3, respectively, on the same strike-slip fault with identical velocity structure. (a, b) Near-fault surface velocity magnitude during the propagation of (a) sub-Rayleigh and (b) supershear rupture. The emergence of Mach front clearly extends the ground shaking to further distance. (c,d) Shake maps with the modified Mercalli intensity (MMI) for (c) sub-Rayleigh and (b) supershear earthquakes. Supershear ruptures lead to larger shaking intensities over broader areas. The dynamic rupture simulations are generated by solving both the elastodynamics and frictional response on the fault. The frictional behavior is governed by linear slip weakening. Nucleation of the rupture is achieved by using a time-weakening friction within a circular patch of radius r = 3 km. The normal stress varies along depth due to difference between overburden stress and the hydrostatic pore pressure. The initial shear stress varies proportionally with the normal stress to achieve either a subshear or supershear rupture propagation. The implementation details follow Abdelmeguid *et al.* (2025). The color version of this figure is available only in the electronic edition.

ground-motion models strive to include all recorded data, there is a significant gap in the available datasets for large earthquakes in the near-fault regions (up to 20–30 km; Abrahamson *et al.*, 2014; Boore *et al.*, 2014). This is an impediment to distinguishing between ground-motion features of supershear and subshear events including orientational directivity and attenuation effects. Given that 70% of the population in California lives within 30 miles of a major active fault, this sparsity of data—specially for supershear events—limits our ability to accurately estimate the hazard levels.

Global Evidence is Clear

Over the past three decades, an increasing number of large strike-slip earthquakes have demonstrated the occurrence of supershear ruptures accompanied by unusually intense shaking and widespread destruction. Supershear ruptures were initially hypothesized in theoretical studies in the mid 1970s (Burridge, 1973; Andrews, 1976; Das and Aki, 1977; Freund, 1979) and then gained empirical evidence through laboratory experiments in 1999 (Rosakis *et al.*, 1999). The experimental breakthrough prompted seismologists to accept the possibility of supershear and to look for observable signatures. In seismic records, supershear ruptures can be identified through a fast rupture arrival phase (Yao and Yang, 2025), or a dominant fault parallel motion using near-fault records (Dunham and Archuleta, 2004; Mello *et al.*, 2014; Rosakis *et al.*, 2025). However, such data are usually limited except in very rare circumstances such as the M_w 7.8 Türkiye earthquake due to the sparsity of near-fault seismic records. Prolonged supershear rupture speeds can also be identified in the far-field through their unique Rayleigh Mach waves signature (Vallée and Dunham, 2012), or using backprojection approaches that time-reverse recorded waves to identify the location and timing of energy release from earthquake ruptures (Bao *et al.*, 2019).

Three notable examples of highly destructive supershear earthquakes include: the 1999 M_w 7.6 İzmit, Türkiye, earthquake with 17,000 reported fatalities and half a million displaced people; the devastating 2018 M_w 7.5 Palu (Sulawesi), Indonesia, earthquake which, along with its tsunami, killed 4300 people, injured 11,000, and displaced over 200,000, and more recently, the catastrophic 6 February 2023 M_w 7.8 Pazarcik earthquake

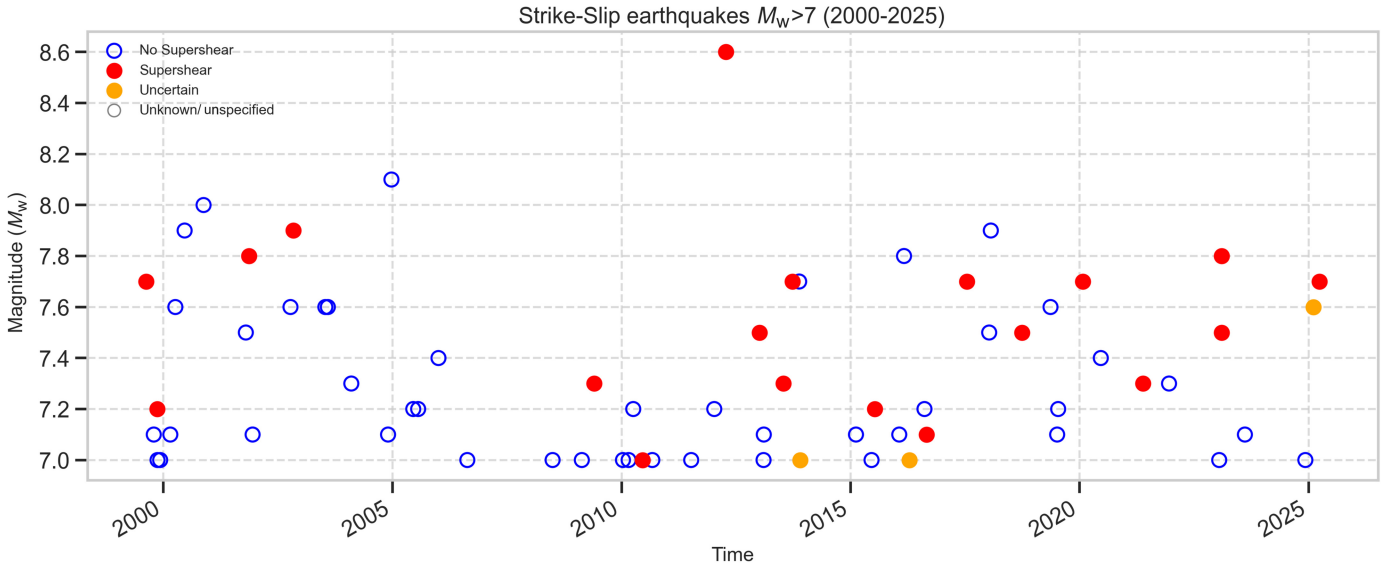

Figure 2. Earthquakes with $M_w > 7.0$ that occurred on strike-slip faults during the period 1999–2025. Open-blue circles represent sub-Rayleigh events. Filled-red circles represent supershear events. Filled-orange circles represent events that are suspected to be supershear but the evidence is not conclusive. The color version of this figure is available only in the electronic edition.

along the East Anatolian fault. This event was triggered by a supershear rupture along a splay fault and exhibited supershear propagation across multiple segments of its 300 km rupture path, with particularly destructive effects near Antakya. The Kahramanmaraş sequence resulted in more than 59,000 confirmed deaths, making it the fifth deadliest earthquake of the twenty-first century with damage exceeding $118.8 billion. These example earthquakes contributed to our understanding of supershear ruptures and highlighted the catastrophic consequences when preparedness is lacking. An extended list of $M_w > 7$ strike-slip supershear events between 1999, the year marking the experimental demonstration of supershear propagation, and 2025 is provided in the following dataset (Elbanna *et al.*, 2025).

Among the 67 $M_w > 7.0$ cataloged earthquakes that occurred on strike-slip faults since 1999, 19 events have been identified (Fig. 2) as supershear, including the most recent M_w 7.7 Mandalay earthquake in Burma (Myanmar). In the past 15 yr, 14 out of 39 large strike-slip earthquakes (~36%) exhibited features of supershear ruptures. This high rate of reported supershear events suggests (1) the acceptance of the supershear phenomenon by the seismological community and (2) that the ongoing expansion and densification of global seismic networks, especially near major known faults, have significantly enhanced our ability to detect supershear phenomena (although much more still needs to be done as discussed later). Indeed, prior to 1999, there was only a single report of episodic supershear rupture in relation to the Imperial Valley earthquake (Archuleta, 1984). Revisiting some historic large events, such as the 1906 San Francisco earthquake, has also suggested likely supershear rupture speeds (Song *et al.*, 2008). Although previous studies provided evidence that supershear earthquakes are more frequent than once thought (e.g., Bao *et al.*, 2022), our updated analysis highlights further the increased frequency of occurrence of supershear earthquakes of M_w 7.0+ which are most relevant to regions like California. For example, in the last 3 yr, four out of six large earthquakes on strike-slip faults are classified as supershear events. Nonetheless, the topic remains underexplored in geotechnical and structural earthquake engineering literature and designs standards.

A Threat at Home: California's Supershear-Ready Faults

Nowhere in the United States is this threat more relevant than in California. The San Andreas fault, the San Jacinto fault, the Newport–Inglewood fault, the Calaveras fault, the Hayward fault, and many others slice through or near major metropolitan areas such as Los Angeles and the San Francisco Bay Area, and are capable of generating earthquakes with $M_w \geq 7.0$. Numerical simulations, including those conducted by the Southern California Earthquake Center (SCEC) and partners (SCEC article number 1003; Elbanna *et al.*, 2023) using the CyberShake platform (Callaghan *et al.*, 2024), illustrate potential seismic hazards from earthquakes in these faults. Example simulations modeling a rupture propagating toward Los Angeles, estimated peak ground velocities exceeding 2 m/s in the forward direction and peak ground accelerations approaching 1.8*g* near the fault. Importantly, these values were generated by assuming classical sub-Rayleigh ruptures. Given that supershear ruptures produce Mach waves and enhanced forward rupture directivity in the fault-parallel direction, it is likely that the ground motions in a supershear scenario could

exceed these already high estimates. Although California building codes are generally more conservative than other national and international design standards, the explicit evaluation of increased shaking intensity in near-fault regions prone to supershear shaking remains necessary. The lack of direct measurements makes the reliance on empirical estimates insufficient, and estimates of uncertainties might be high. Potentially elevated shaking intensity could increase the expected risk for large areas surrounding the large faults. In addition, elevated strong shaking may enhance triggering cascading secondary hazards including landslides in steep terrains, liquefaction in basin fill regions, surface fault rupture, and fire outbreaks due to utility failures. Supershear ruptures on partially submerged faults near the coast line may also contribute to generation of local tsunamis (Elbanna *et al.*, 2021).

A Call to Action

The threat of supershear earthquakes is well documented, and likely to occur along major strike-slip faults in California, compounding seismic hazards from large events near major metropolitan areas. Although prominent planning activities, including ShakeOut scenarios, have traditionally focused on classic, sub-Rayleigh ruptures, there is a clear opportunity to further strengthen our preparedness by explicitly incorporating the amplified hazards posed by supershear events. It is imperative that we update these scenarios to account for supershear ruptures and their associated elevated shaking in hazard estimates including quantifying the expanded footprint of cascading secondary hazards. Supershear ruptures also pose a significant challenge to earthquake early warning systems like ShakeAlert, which rely on detecting the arrival of fast-moving P waves and estimating the magnitude and intensity of shaking before the onset of damaging S waves to issue alerts. In supershear events, for which rupture speed may approach the P-wave speed soon after nucleation, this delay can become very small—especially in the rupture's forward direction where most seismic energy is concentrated. As a result, communities within the strongest shaking area surrounding the fault may receive little or no warning before intense, shock-wave dominated shaking arrives. Furthermore, earthquake magnitude or extent of rupture may be underestimated initially if transition to supershear is not accounted for. It is therefore essential to incorporate supershear rupture dynamics into the training and testing of early warning algorithms. We must also reassess the vulnerability of infrastructure and update the relevant building code provisions—especially for critical facilities that lie within expected forward rupture corridors—under these more intense loading conditions. This is especially true for nuclear and hydropower plant equipment, which are most sensitive to high frequencies ($f > 3$ Hz) that are amplified by the shock wavefronts.

We call for systematic interdisciplinary investigations—through field observation, simulation, and structural response analysis—of how supershear effects impact the built environment. We advocate for a research and a science-based policy agenda that would

1. improve observational coverage near known strike-slip faults: although the combined evidence for supershear ruptures from the so-far documented events is clear, they were mostly recorded with very sparse sensors near the faults, significantly limiting the information and insights that detailed recordings could have provided. Dense arrays of sensors across hazardous faults will allow recording near-fault data from future large earthquakes, which can revolutionize the state of knowledge about earthquake processes and significantly improve the mitigation of seismic risks through data analyses, computation, and model development (Ben-Zion, 2019);
2. develop physics-based ground-motion simulations for supershear scenarios with realistic fault geometries and velocity structures. This requires resolving many outstanding questions on supershear rupture dynamics and the interactions with the shallow geotechnical layer (Abdelmeguid *et al.*, 2025; Hu *et al.*, 2020), including how shock waves amplify and internally reflect within sedimentary basins and fault damage zones, as well as implications for extended shaking duration. Advanced computational modeling along with analog experiments that generate laboratory ruptures in a controlled environment are critically needed to uncover consequential supershear rupture details that remain elusive for direct field observations;
3. assess structural response under aggregated simulated and observed supershear ground motions: having synthetic ground-motion data from near-fault sites will complement existing sparse observational datasets and enable us to accurately model the structural response of built environment under supershear excitations to better understand its implications;
4. evaluate when and how to include the effects of supershear ruptures in seismic hazard models and design guidelines: the results of these studies would inform discussion on code modifications, hazard modeling, and risk assessment; and
5. raise awareness among different stakeholders: beyond improving observations, modeling and analysis, we need strategic investments in mitigation, ranging from retrofitting at-risk structures to refining emergency response protocols. Earthquake education and preparedness efforts should evolve to engage stakeholders across the spectrum including earthquake scientists and engineers, social scientists, psychologists, economists, emergency managers, and policy makers, to improve the preparedness of communities to realistic earthquake hazards.

Data and Resources

The full earthquake catalog used was obtained from U.S. Geological Survey (2025). Both the full and processed catalog can be obtained at Elbanna *et al.* (2025). The sub-Rayleigh and supershear ruptures in

Figure 1 are simulated using DRDG3D (Zhang *et al.*, 2023), which is an open-source software.

Declaration of Competing Interests

The authors acknowledge that there are no conflicts of interest recorded.

Acknowledgments

The authors are grateful to the anonymous reviewer for their constructive comments, which helped improve the manuscript.

References

Abdelmeguid, M., A. Elbanna, and A. Rosakis (2025). Ground motion characteristics of subshear and supershear ruptures in the presence of sediment layers, *Geophys. J. Int.* **240,** no. 2, 967–987.

Abrahamson, N. A., W. J. Silva, and R. Kamai (2014). Summary of the ASK14 ground motion relation for active crustal regions, *Earthq. Spectra* **30,** no. 3, 1025–1055.

Andrews, D. (1976). Rupture velocity of plane strain shear cracks, *J. Geophys. Res.* **81,** no. 32, 5679–5687.

Archuleta, R. J. (1984). A faulting model for the 1979 Imperial Valley earthquake, *J. Geophys. Res.* **89,** no. B6, 4559–4585.

ASCE/SEI (2022). *Minimum Design Loads and Associated Criteria for Buildings and Other Structures*, American Society of Civil Engineers, Reston, Virginia.

Bao, H., J.-P. Ampuero, L. Meng, E. J. Fielding, C. Liang, C. W. Milliner, T. Feng, and H. Huang (2019). Early and persistent supershear rupture of the 2018 magnitude 7.5 Palu earthquake, *Nature Geosci.* **12,** no. 3, 200–205.

Bao, H., L. Xu, L. Meng, J. P. Ampuero, L. Gao, and H. Zhang (2022). Global frequency of oceanic and continental supershear earthquakes, *Nature Geosci.* **15,** no. 11, 942–949.

Ben-Zion, Y. (2019). A critical data gap in earthquake physics, *Seismol. Res. Lett.* **90,** no. 4, 1721–1722.

Boore, D. M., J. P. Stewart, E. Seyhan, and G. M. Atkinson (2014). NGA-West2 equations for predicting PGA, PGV, and 5% damped PSA for shallow crustal earthquakes, *Earthq. Spectra* **30,** no. 3, 1057–1085.

Burridge, R. (1973). Admissible speeds for plane-strain self-similar shear cracks with friction but lacking cohesion, *Geophys. J. Int.* **35,** no. 4, 439–455.

Callaghan, S., P. J. Maechling, F. Silva, M.-H. Su, K. R. Milner, R. W. Graves, K. B. Olsen, Y. Cui, K. Vahi, A. Kottke, *et al.* (2024). Using open-science workflow tools to produce SCEC cybershake physics-based probabilistic seismic hazard models, *Front. High Perform. Comput.* **2**, 1360720, doi: 10.3389/fhpcp.2024.1360720.

Das, S., and K. Aki (1977). A numerical study of two-dimensional spontaneous rupture propagation, *Geophys. J. Int.* **50,** no. 3, 643–668.

Dunham, E. M., and R. J. Archuleta (2004). Evidence for a supershear transient during the 2002 Denali fault earthquake, *Bull. Seismol. Soc. Am.* **94,** no. 6B, S256–S268.

Dunham, E. M., and H. S. Bhat (2008). Attenuation of radiated ground motion and stresses from three-dimensional supershear ruptures, *J. Geophys. Res.* **113,** no. B8, doi: 10.1029/2007JB005182.

Elbanna, A., M. Abdelmeguid, D. Asimaki, N. Tainpakdipat, G. Lavrentiadis, A. Rosakis, and Y. Ben-Zion (2025). Supershear earthquakes: A global wake-up call we can't afford to ignore, *Zenodo*, doi: 10.5281/zenodo.15185767.

Elbanna, A., M. Abdelmeguid, X. Ma, F. Amlani, H. S. Bhat, C. Synolakis, and A. J. Rosakis (2021). Anatomy of strike-slip fault tsunami genesis, *Proc. Natl. Acad. Sci.* **118,** no. 19, e2025632118, doi: 10.1073/pnas.2025632118.

Elbanna, A., K. Milner, and Y. Ben-Zion (2023). *The 2023 Kahramanmaras earthquake sequence in Turkey: Relations to California earthquakes, ground motion, and seismic risk*, SCEC, Los Angeles, California, SCEC contribution #12730, available at https://www.scec.org/article/1003 (last accessed July 2025).

Freund, L. (1979). The mechanics of dynamic shear crack propagation, *J. Geophys. Res.* **84,** no. B5, 2199–2209.

Hu, F., D. D. Oglesby, and X. Chen (2020). The near-fault ground motion characteristics of sustained and unsustained free surface-induced supershear rupture on strike-slip faults, *J. Geophys. Res.* **125,** no. 5, e2019JB019039, doi: 10.1029/2019JB019039.

Mello, M., H. Bhat, A. Rosakis, and H. Kanamori (2010). Identifying the unique ground motion signatures of supershear earthquakes: Theory and experiments, *Tectonophysics* **493,** nos. 3/4, 297–326.

Mello, M., H. Bhat, A. Rosakis, and H. Kanamori (2014). Reproducing the supershear portion of the 2002 Denali earthquake rupture in laboratory, *Earth Planet. Sci. Lett.* **387,** 89–96.

Rosakis, A., M. Abdelmeguid, and A. Elbanna (2025). Near-field evidence for early supershear rupture of the Mw 7.8 Kahramanmaraş earthquake in Turkey, *Nature Geosci.* **18,** no. 6, 534–541.

Rosakis, A., O. Samudrala, and D. Coker (1999). Cracks faster than the shear wave speed, *Science* **284,** no. 5418, 1337–1340.

Song, S. G., G. C. Beroza, and P. Segall (2008). A unified source model for the 1906 San Francisco earthquake, *Bull. Seismol. Soc. Am.* **98,** no. 2, 823–831.

U.S. Geological Survey (2025). *Earthquake lists, maps, and statistics*, *Technical Rept. U.S. Geol. Surv*, available at https://earthquake.usgs.gov/earthquakes (last accessed April 2025).

Vallée, M., and E. M. Dunham (2012). Observation of far–field mach waves generated by the 2001 Kokoxili supershear earthquake, *Geophys. Res. Lett.* **39,** no. 5, doi: 10.1029/2011GL050725.

Yao, S., and H. Yang (2025). Rupture phases reveal geometry-related rupture propagation in a natural earthquake, *Sci. Adv.* **11,** no. 4, eadq0154, doi: 10.1126/sciadv.adq0154.

Zhang, W., Y. Liu, and X. Chen (2023). A mixed-flux-based nodal discontinuous Galerkin method for 3d dynamic rupture modeling, *J. Geophys. Res.* **128,** no. 6, e2022JB025817, doi: 10.1029/2022JB025817.

Manuscript received 11 April 2025
Published online 19 August 2025